

Impact of a Superhydrophobic Sphere onto Water

Duck-Gyu Lee and Ho-Young Kim*

School of Mechanical and Aerospace Engineering, Seoul National University, Seoul 151-744, Korea

Received August 8, 2007. In Final Form: September 19, 2007

When a water drop hits a superhydrophobic solid surface, it bounces off the substrate like an elastic ball. Here we show that when a tiny superhydrophobic solid sphere impacts with water, it can bounce off the free surface just as it impacts with an elastic membrane. The motion of a sinking sphere is analytically calculated by solving a potential flow whose free boundary is determined by the Young–Laplace equation. To find conditions under which the solid sphere should sink, bounce off, or oscillate upon impact with water, we construct simple scaling laws which are shown to agree well with experimentally found boundaries between the distinct impact behaviors in a regime map based on dimensionless parameters.

Introduction

Motion of small objects floating on a liquid surface is a subject of recently growing interest due to its relevance with water-walking insects^{1,2} and self-assembly using capillary forces.³ In particular, insects such as water striders and fishing spiders adopt surprisingly versatile ways of moving on water, including skating, meniscus climbing, and jumping.² Our study was initially motivated by those insects that can jump on water without being drowned. Water strider legs were shown to be strongly water repellent due to a hierarchical structure of hydrophobic hairs on the legs,⁴ and such superhydrophobicity is assumed to enable or greatly facilitate the agile motions of the insects.

To obtain a basic understanding of the dynamics behind such insects' locomotion on water, we have investigated behavior of hydrophobic solids interacting with free surface of water. We showed earlier that tiny hydrophobic objects can float on water even when they are denser than water, owing to the vertical component of capillary force.⁵ Also the sinking of even denser objects was shown to be retarded by the capillary force when in contact with deforming meniscus.⁶ Although not solid, a liquid marble, a water drop coated with hydrophobic grains, was shown to float on water for a considerably long time.⁷ A numerical computation was made for a simplified model of a jumping water strider having a spring supporting a point mass.⁸ In this work, we experimentally observe tiny superhydrophobic spheres impact with water to discover three distinct impact behavior, i.e., damped oscillation, complete bouncing-off, and sinking, as shown in Figure 1, depending on impact conditions. We theoretically analyze the initial sinking motion of the sphere by combining a potential flow theory and the Young–Laplace equation. Scaling laws are then constructed to predict the conditions that determine the impact behavior of the sphere, which leads to a regime map in a space of dimensionless parameters.

Dimensional Analysis and Experiments

When a solid sphere of radius R and density ρ_s impacts with the velocity U onto the surface of liquid having density ρ_f , surface tension

γ and viscosity μ , the sphere experiences various forces while interacting with the liquid and its interface. The forces include the solid weight ($\sim -\rho_s g R^3$), buoyancy ($\sim \rho_f g R^3$), added inertia ($\sim \rho_f R^3 \dot{h}$), form drag ($\sim \rho_f h^2 R^2$), viscous force ($\sim \mu h R$) and surface tension ($\sim \gamma R$).² Here the negative sign indicates the direction of gravity, h denotes the location of sphere's center, being positive when upward and zero at the undisturbed free surface, and $\dot{h} \equiv dh/dt$, with t being time. The equation of motion for the sphere is obtained by equating the sphere inertia ($\rho_s R^3 \dot{h}$) to the sum of the above forces. Dimensional analysis can simplify this physical picture, leading to the following relationship:

$$\frac{h}{l_c} = f(D, \text{Bo}, \text{We}, \text{Re}, \theta) \quad (1)$$

where the capillary length $l_c = \sqrt{\gamma/\rho_f g}$, the density ratio $D = \rho_s/\rho_f$, the Bond number $\text{Bo} = \rho_f g (2R)^2/\gamma$, the Weber number $\text{We} = \rho_f U^2 (2R)/\gamma$, the Reynolds number $\text{Re} = \rho_f U (2R)/\mu$, and θ is the contact angle. In a case where the Reynolds number is very high, the viscous effects can be ignored and, thus, the impact behavior of superhydrophobic spheres (θ fixed) can be determined by the three dimensionless parameters of D , We , and Bo .

We performed experiments to investigate the effects of the foregoing parameters on the sphere's impact behavior. We used spheres with $0.67 \text{ mm} < R < 1 \text{ mm}$ made of various materials including glass, PC (polycarbonate), PP (polypropylene), POM (polyoxymethylene), PTFE (polytetrafluoroethylene), PVDF (polyvinylidene fluoride), and aluminum to obtain a wide range of density ratio, $0.88 < D < 2.48$. The spheres were coated with mixture of AKD (alkyl ketene dimer) and chloroform to turn superhydrophobic with the contact angle of 154° with water. Figure 2 shows images of a water drop placed on a flat surface treated as described above and of a treated sphere floating on water. In the experiments, we dropped spheres of various density from different heights onto water to vary the impact velocity from 0.45 to 1.81 m/s. A high-speed camera recorded the impact process of the spheres at the rate of 3000 frames per second.

Hydrodynamic Theory

As mentioned earlier, we found three distinct types of impact behavior of the superhydrophobic spheres. Although our spheres varied in density, all of them were able to float due to its hydrophobicity if gently placed on water.⁵ When the sphere hits the water surface with a low velocity, it merely oscillates on the surface while being afloat. As the impact velocity increases, the

* To whom correspondence should be addressed. E-mail: hyk@snu.ac.kr.

- (1) Hu, D. L.; Chan, B.; Bush, J. W. M. *Nature* **2003**, *424*, 663–666.
- (2) Bush, J. W. M.; Hu, D. L. *Annu. Rev. Fluid Mech.* **2006**, *38*, 339–369.
- (3) Vella, D.; Mahadevan, L. *Am. J. Phys.* **2005**, *73*, 817–825.
- (4) Gao, X.; Jiang, L. *Nature* **2004**, *432*, 36.
- (5) Vella, D.; Lee, D.-G.; Kim, H.-Y. *Langmuir* **2006**, *22*, 5979–5981.
- (6) Vella, D.; Lee, D.-G.; Kim, H.-Y. *Langmuir* **2006**, *22*, 2972–2974.
- (7) Aussillous, P.; Quéré, D. *Proc. R. Soc. A* **2006**, *462*, 973–999.

(8) Li, J.; Hesse, M.; Ziegler, J.; Woods, A. W. *J. Comp. Phys.* **2005**, *208*, 289–314.

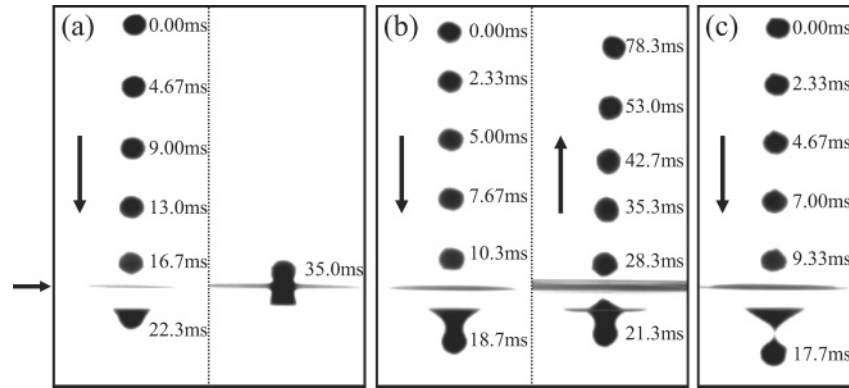


Figure 1. Three distinct types of impact behavior of a superhydrophobic sphere on water. The vertical arrows indicate the direction of sphere motion, and the horizontal arrow the location of the undisturbed free surface. (a) Damped oscillation without losing contact with free surface ($\rho_s = 615 \text{ kg/m}^3$, $U = 1.23 \text{ m/s}$, $R = 0.98 \text{ mm}$). (b) Bouncing-off ($\rho_s = 654 \text{ kg/m}^3$, $U = 1.84 \text{ m/s}$, $R = 0.96 \text{ mm}$). (c) Sinking ($\rho_s = 649 \text{ kg/m}^3$, $U = 1.93 \text{ m/s}$, $R = 0.97 \text{ mm}$).

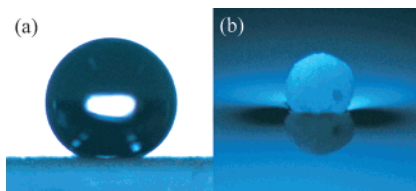


Figure 2. Images of (a) a 0.49-mm-radius water drop on the superhydrophobic surface and (b) a 0.84-mm-radius superhydrophobic sphere with $D = 0.972$ on water.

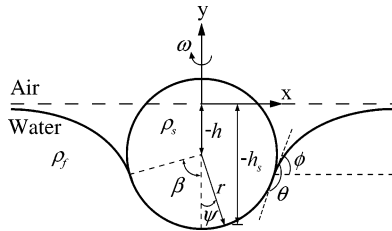


Figure 3. Geometry of a sphere lying at the interface between a liquid and a gas.

oscillation amplitude first increases. However, further increase in the impact velocity makes the sphere completely bounce off the water surface. As the impact velocity increases even more, however, the sphere completely penetrates the interface and sinks.

In all the three cases, initial sinking is ubiquitous while the presence and strength of subsequent rebound distinguishes the eventual behavior. Hence, we first consider a simple hydrodynamic theory which enables us to calculate the forces acting on a sphere and its velocity during initial sinking while the sphere is still in contact with the gas/liquid interface. We follow a similar reasoning adopted for modeling a sinking cylinder.⁶ In our experiments, the Reynolds number based on the initial impact speed was typically on the order of 10^2 – 10^3 . We assume that the flow induced by an impacting sphere is potential flow, so that the velocity potential φ around the sphere may be written as $\varphi = \dot{h}R^3 \cos \psi / 2r^2$. Here φ is defined by $\mathbf{u} = \nabla \varphi$, where \mathbf{u} being the velocity field, (r, ψ, ω) is a spherical coordinate system as shown in Figure 3, \dot{h} is a velocity of the sphere and ψ is the angle between the negative y direction and the radial vector \mathbf{r} .⁹ Due to axisymmetry of the flows, there is no dependency on ω . Since

the flows induced by the impacting sphere are accelerating, we use an unsteady Bernoulli equation:

$$\frac{\partial \varphi}{\partial t} + \frac{p}{\rho_f} + \frac{1}{2} |\nabla \varphi|^2 + gh = F(t) \quad (2)$$

where p is the pressure and $F(t)$ is an arbitrary function of time alone. The pressure at $r = R$ and $\psi = \beta$ is the atmospheric pressure p_a , which gives $F(t)$ as

$$F(t) = \frac{R}{2} \ddot{h} \cos \beta - \frac{9}{8} \dot{h}^2 \cos^2 \beta + \frac{p_a}{\rho_f} + \frac{5}{8} \dot{h}^2 \quad (3)$$

The pressure distribution around the sphere is given by

$$p(R, \psi) = p_a - \rho_f g h_s + \frac{\rho_f R}{2} \ddot{h} (\cos \beta - \cos \psi) + \frac{9}{8} \dot{h}^2 (\cos^2 \psi - \cos^2 \beta) \quad (4)$$

where $h_s = h - R \cos \psi$. This then allows us to calculate the vertical component of the pressure force acting on the sphere as

$$F_p = -\frac{\pi}{6} R^3 \rho_f \dot{h} A(\beta) + \frac{9\pi}{16} R^2 \rho_f \dot{h}^2 \sin^4 \beta + \frac{\pi}{3} R^2 \rho_f g B(\beta, h) \quad (5)$$

where $A(\beta) = (\cos^3 \beta - 3 \cos \beta + 2)$ and $B(\beta, h) = (3h \cos^2 \beta - 2R \cos^3 \beta - 3h + 2R)$. The first term on the right-hand side of eq 5 represents the added inertia induced by the flows around the accelerating sphere, the second term the form drag, and the last term the buoyancy. Now we get the following equation of motion for the sphere:

$$\frac{4}{3} \pi R^3 \rho_s \ddot{h} = F_p - \frac{4}{3} \pi R^3 \rho_s g + 2\pi R \gamma \sin \beta \sin \phi \quad (6)$$

where the second term on the right-hand side of eq 6 is the sphere weight and the third term the vertical component of the surface tension force. Equation 6 can be solved once the values of β and ϕ are determined. We determine the angle β as a function of h by solving the Young–Laplace equation, which is assumed to hold for a deforming interface,⁶ and then ϕ by the geometric condition, $\phi = \theta + \beta - \pi$. We can solve eq 6 numerically with two initial conditions, the initial position of the sphere's center h and the initial velocity of a sphere \dot{h} which are provided by experiments.

(9) Currie, I. G. *Fundamental Mechanics of Fluids*; Marcel Dekker: New York, 2003.

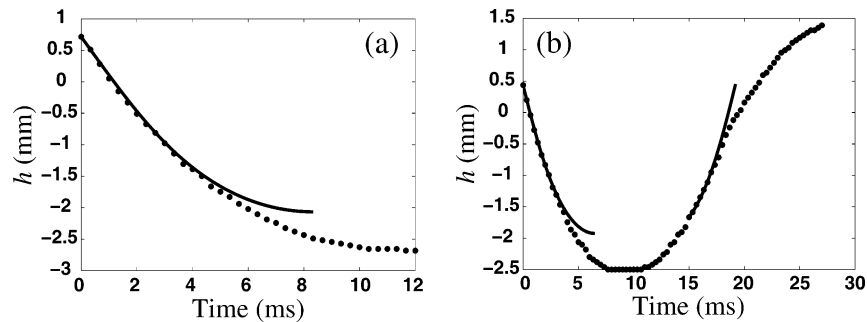


Figure 4. Comparison between theoretical predictions (solid lines) and experimental results (filled circles) of the locations of (a) a sinking sphere ($\rho_s = 1990 \text{ kg/m}^3$, $U = 0.73 \text{ m/s}$, $R = 0.87 \text{ mm}$) and (b) a bouncing sphere ($\rho_s = 1320 \text{ kg/m}^3$, $U = 0.89 \text{ m/s}$, $R = 0.96 \text{ mm}$). For each computation, initial velocity was obtained using first two measured locations of the sphere.

Figure 4a shows the temporal evolution of the location of a sphere that completely sinks into water upon impact. It reveals good agreement between experiment and theory in the initial stages where the meniscus deformation is mild, so that our assumptions of the velocity profile and the Young–Laplace equation remain valid. The theory agrees with the experimental results even when the sphere bounces off, as in Figure 4b in both the early impact and early rebounding stages.

Scaling Laws

Although our simple hydrodynamic theory captures essential physics of sinking and bouncing, it has a limitation in solving the sphere motion near zero velocity; thus, it is unable to accurately predict whether the sphere will bounce back or completely sink. In the meantime, scaling laws to determine impact behavior can be constructed by simple force balance, and they are corroborated experimentally in the following. First, we consider a physical criterion that determines whether the sphere will completely sink or bounce. It is obvious that the sphere can bounce upward (or the direction of motion is reverted) only after the downward velocity of the sphere reduces to zero. Otherwise, the sphere keeps falling due to persisting downward velocity. This leads to a criterion that the deceleration during initial sinking should be large enough to make the sphere velocity zero for bouncing to occur.¹⁰

The deceleration is caused by such forces as added inertia, buoyancy, form drag, and surface tension. By computing the contribution of each force component using the theory presented above, we find that the surface tension is a dominant force as shown in Figure 5. To evaluate the magnitude of the viscous force ignored in the theory, we consider a ratio of the viscous force to surface tension, i.e., the capillary number $Ca = \mu v / \gamma$, where v is the velocity. Although v is fairly small compared with the impact velocity U , using U in evaluating Ca yields about 0.1 in our cases, indicating still dominant contribution of surface tension over viscosity.

Balancing the solid inertia ($\sim \rho_s R^3 a_s$) with surface tension ($\sim \gamma R$) gives the scale of deceleration during sinking, $a_s \sim \gamma / \rho_s R^2$. Here we note that when the sphere experiences the maximum upward force due to surface tension, the meniscus shape is such that $\phi = \theta/2$,⁵ where ϕ is the angle of inclination of the interface to the horizontal as shown in Figure 3, leading to a simple scaling for the surface tension force ($\sim \gamma R$). The time scale of the initial sinking process, t_c , is given by the time for the capillary-gravity wave to travel the capillary length $l_c \equiv (\gamma / \rho g)^{1/2}$, thus $t_c = (\gamma / \rho g^3)^{1/4}$.⁶ For the sphere to reach zero velocity, the characteristic sinking velocity, U_s , which is scaled as $U_s \sim U$, as verified in

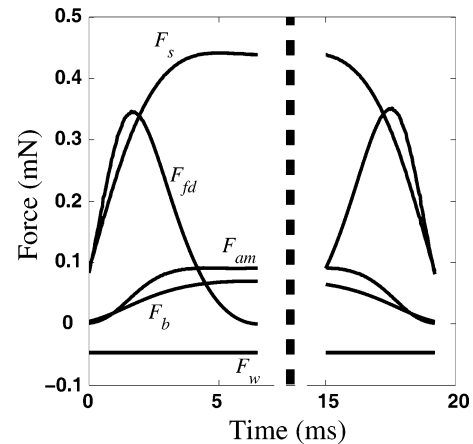


Figure 5. Contribution of each force component appearing in eqs 5–6 exerted on a sphere that bounces off. F_s denotes the magnitude of surface tension force, F_{fd} form drag, F_{am} added mass, F_b buoyancy, and F_w weight.

Figure 6a, should be balanced with the velocity decrement for t_c , thus $U \sim a_s t_c$. Here U_s and U_b , the characteristic bouncing velocity as will be used below, are determined as the average velocity in the time range where h varies linearly with time. Rearrangement yields the following dimensionless relationship that determines the boundary between the sinking and the bouncing behaviors: $WeBo^{3/2} \sim D^{-2}$.

Once the sphere rebounds upon initial sinking, it either completely bounces off the water surface or merely oscillates without losing contact with the free surface. This is determined by whether the sphere's upward rebound velocity decreases to zero while the meniscus contacts the rising sphere (damped oscillation) or it retains nonzero up velocity until the sphere leaves the free surface (complete bouncing-off). After the sphere reverts its direction of motion from initial sinking, its rebound velocity can be scaled as the impact velocity ($U_b \sim U$). This is supported by observing that the temporal evolution of h during rebound is almost symmetrical to that during sinking as shown in Figure 4b. Thus, the time scale of the bouncing can be taken as t_c because capillary-gravity wave needs to travel back the similar distance as before, l_c . This was verified by experiments as shown in Figure 6b. Observing the right half of Figure 5 reveals that the surface tension is again the dominant force to pull the rebounding sphere down. Thus, we get the same order of magnitude of deceleration for this rebound motion as above, $a_b \sim \gamma / \rho_s R^2$. The sphere completely bounces off unless the rebound velocity of the sphere decreases to zero for the time of the order of t_c . Therefore, the boundary between the complete bouncing-off and the damped oscillation is given by the balance $U \sim a_b t_c$, which leads to $WeBo^{3/2} \sim D^{-2}$.

(10) No spheres were observed to sink back once they started to rebound upon hitting zero velocity.

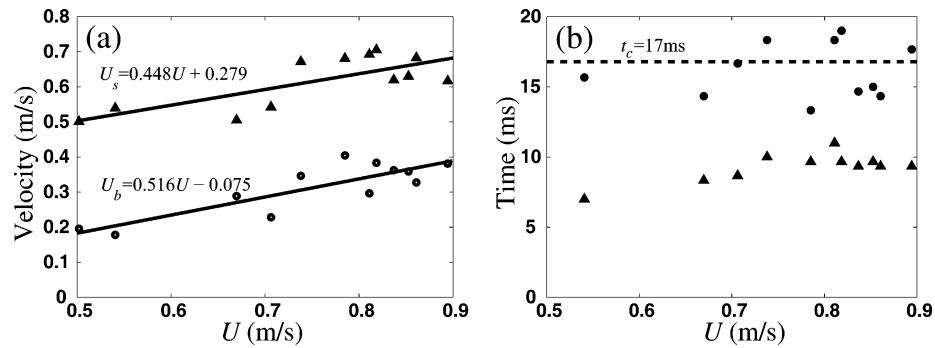


Figure 6. (a) Relationship of U_s and U_b with impact velocity. (b) Times taken for a sphere to sink (circles) and bounce (triangles) when the density ratio of the spheres varies as $1.3 < D < 1.5$.

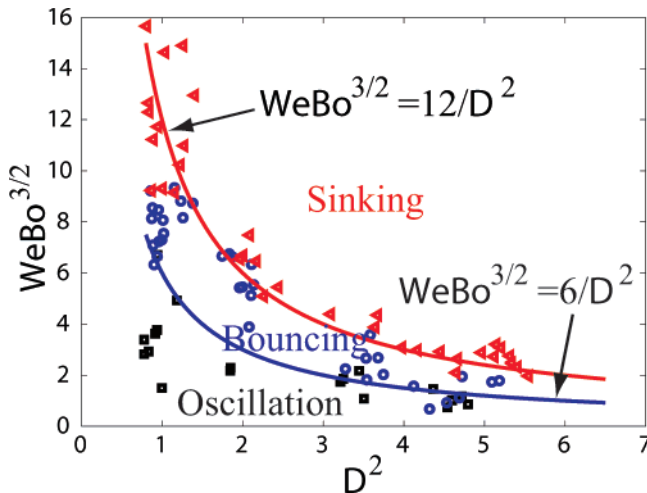


Figure 7. (Color online) Regime map for impact behavior of superhydrophobic spheres. The lines are drawn following the scaling laws with prefactors determined empirically. Triangles, circles, and squares represent the experimental conditions for sinking, bouncing, and oscillation, respectively.

Figure 7 shows a regime map for sphere impact behavior based on the scaling laws. The ordinate roughly measures the ratio of inertia imparted to the liquid to the surface tension. The experimental data indicating the boundaries between the three distinct types of impact behavior match reasonably well with the scaling laws. Our scaling laws signify that low-density superhydrophobic spheres are very likely to bounce even when they impact with high inertia. However, high-density superhydrophobic spheres can float only when the impact occurs mildly.

Discussions and Conclusions

We note that the regime map was constructed using three dimensionless parameters (D , Bo , and We), which could be

justified for impacts of sub-millimeter-sized superhydrophobic objects with the velocity of the order of 1 m/s onto water. Especially we reported the “bouncing” behavior of a solid object, which is peculiar to a superhydrophobic impact onto a liquid with a low viscosity. To investigate the effects of viscosity, we performed experiments to find the critical viscosity over which the bouncing motion disappears in the dynamic impact conditions as covered by Figure 7. By using mixtures of water and ethylene glycol, we found that the superhydrophobic spheres either completely sink or oscillate without bouncing off when the viscosity reaches ~ 3 mPa·s, three times larger than that of pure water. The similar observation of the absence of complete bouncing-off was made when less hydrophobic spheres ($\theta = 104^\circ$) impacted with water in the identical range of dynamic impact conditions.

The highly improved ability of heavy hydrophobic solids to keep afloat on water even after impacting upon water with a high velocity appears to explain partially why water striders have superhydrophobic legs. Our recent study⁵ revealed that a slightly hydrophobic cylinder (or insect leg) has a similar load-supporting capacity on water to that of a superhydrophobic cylinder in static situations. However, insects having less hydrophobic legs are more likely to drown after jumping, which limits their ability to avoid sudden dangers such as predators.¹¹ Application of our study can be extended to developing semi-aquatic robots that mimic such insects having the surprising mobility on water.

Acknowledgment. We thank D. Vella and Prof. L. Mahadevan for stimulating discussions. This work was supported by a Korea Research Foundation grant (KRF-2006-003-D00068) administered via SNU-IAMD.

LA702437C

(11) Vella, D.; Metcalfe, P. D. *Phys. Fluids* **2007**, *19*, 072108.